COMMUNICATION

Bestowing structure upon the pores of a supramolecular network

Baharan Karamzadeh,[a] Thomas Eaton,[b] Izabela Cebula,[a,c] David Muñoz Torres,[b] Markus Neuburger,[b] Marcel Mayor[*b,d,e] and Manfred Buck[*a]

Trigonal molecules compartmentalise the pores of a honeycomb network of 3,4:9,10-tetracarboxylic diimide (PTCDI) and 1,3,5-triazine-2,4,6-triamine (melamine). Extending the 1,3,5-tri(phenylene-ethynylene)benzene core by a phenyl group allows for a well-defined accommodation of the molecule into two symmetry equivalent positions in the pore. The corresponding styryl or phenylene-ethynylene derivatives exceed the pore size and, thus, impede pore modification.

Supramolecular self-assembly at surfaces represents a convenient route to atomically precise nanostructures.[1] In efforts towards higher complexity and functionality of molecular systems assembly strategies involving more than one or two components[2, 3, 4, 5] can rely on either the simultaneous or sequential assembly of components. Elegantly demonstrated for up to four molecules at the liquid-solid interface,[5] the former relies on the complex interplay of geometrical and energetic factors. Its appeal is the simplicity of assembly in a single step but requires a careful choice of molecules and conditions. The latter approach adopted both for the liquid/solid interface [6-8] and in UHV[2, 9] is more involved but promises larger flexibility as, in particular, different schemes of assembly can be combined[6] or additional processes such as electrochemical deposition[7] or displacement[8] be implemented.

In our studies of hierarchical sequential assembly at the liquid/solid interface as a means to generate ultra-precise nanostructures and approach the ultimate limit in controlling the position of individual molecular entities, a strategy was adopted which is based on the templated assembly of star shaped molecules. Going beyond the formation of homogeneous monolayers of this type of molecules[10, 11] a concept for surface patterning was explored which is complementary to a previously implemented one.[4] Instead of shaping the geometry of the pores of a supramolecular network by modification of a network component, dividing a pore into segments by an additional molecule was investigated. Starting from a honeycomb network which consists of 3,4:9,10-tetracarboxylic diimide (PTCDI) 1,3,5-triazine-2,4,6-triamine

(melamine) and which has been studied both in ultrahigh vacuum (UHV)[12, 13] and under ambient conditions[6, 14, 15], adsorption of a star-shaped molecule is expected to result in a well defined compartmentation of the network pores as illustrated in Fig. 1a.
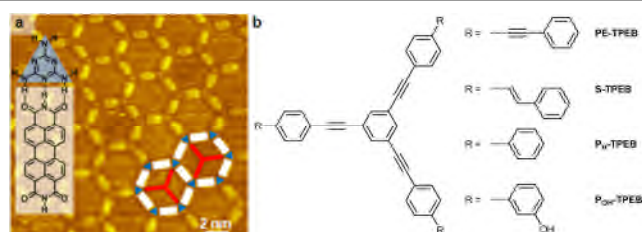

Fig. 1 (a) Melamine (blue triangle) and PTCDI (white rectangle) forming a triple hydrogen bonded honeycomb network as shown in the STM image. (b) Structures of the molecules investigated to sub-divide pores as illustrated in (a) with the red stars representing energetically equivalent positions of the molecules.

To this end differently sized star shaped molecules were investigated consisting of a core of 1,3,5-tri(phenylene ethynylene)benzene (**TPEB**) and various extensions differing in length, namely phenylethynyl (**PE**), styryl (**S**) and phenyl moieties (**P**) (see Fig. 1b). For the latter both the unsubstituted (**P$_H$-TPEB**) and hydroxyl substituted molecules were investigated (**P$_{OH}$-TPEB**).

From simple MM2 force field calculations (see Fig. ESI1) it is expected that **P$_{H/OH}$-TPEB** fits easily into the pore in configurations schematically shown in Fig. 1a. For **S-TPEB** and **PE-TPEB** the situation is less clear. Even though the undistorted molecules exceed the size of the pore, a fit is conceivable due to the considerable flexibility of the ethynylene moiety. While the ethynylene moiety is widely perceived as a rigid linker, significant deviations from linearity by up to 20° have been reported both in bulk and on surfaces[16, 17] which provides additional degrees of freedom for the molecules to be accommodated (see Fig. ESI1). As regards **S-TPEB** and **P$_{OH}$-TPEB** it is noted that these molecule are prochiral. The conformers can exhibit either C_3 symmetry, thus matching the

symmetry of the hexagonal pore, or C_1 symmetry for which, in the case of **S-TPEB**, one arm of the molecule would not point precisely into the direction of a network vertex.
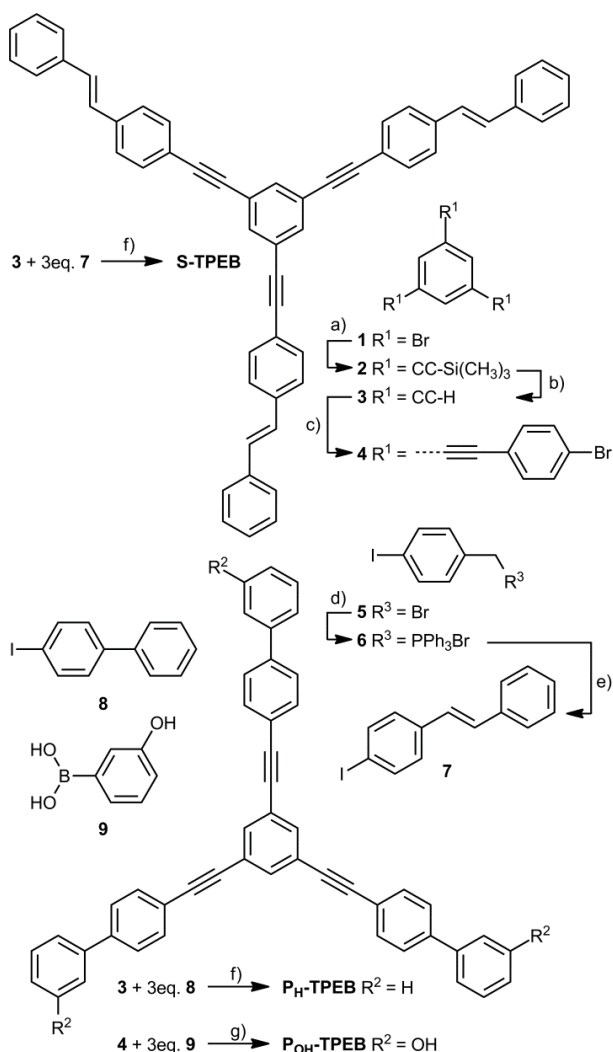
Scheme 1. Synthesis of the molecular stars **S-TPEB**, **P$_H$-TPEB** and **P$_{OH}$-TPEB**. Reagents and conditions: a) TMSA, Pd(PPh$_3$)$_2$Cl$_2$, CuI, THF, iPr$_2$NH, 60°C, 16h, quant.; b) K$_2$CO$_3$, THF, MeOH, r.t., 6h, quant.; c) IC$_6$H$_4$Br, Pd(PPh$_3$)$_2$Cl$_2$, CuI, THF, iPr$_2$NH, r.t., 5h, 79%; d) PPh$_3$, DMF, 85°C, 1h, 76%; e) 1.) toluene, 0°C, tBuOK, C$_6$H$_5$CHO, r.t., 16h, CC; 2.) toluene, cat. I$_2$, rfl., 3h, 77%; f) Pd(PPh$_3$)$_4$, CuI, THF, iPr$_2$NH, r.t., 16h, 49% for **S-TPEB**, 83% for **P$_H$-TPEB**; g) Pd(PPh$_3$)$_4$, K$_2$CO$_3$, toluene, EtOH, micro wave 120°C, 45min., 10%.

The synthesis of the three star-shaped molecules is based on Pd catalyzed cross-coupling chemistry and is sketched in scheme 1.[18] The 1,3,5-triethynylbenzene **3**, as common precursor of **S-TPEB** and **P$_H$-TPEB**, was obtained from 1,3,4-tribromobenzne following a *Sonogashgira* protocol followed by deprotection of the TMS masked ethynyl substituents. The benzylbromide **5** was converted into the *Wittig* salt **6** by treatment with triphenylphosphine. The Wittig reaction with benzaldehyde provided the iodo-functionalized *trans*-stilbene **7** after exposure to reversible iodine addition/elimination conditions. *Sonogashira*–type coupling between the triethynylbenzene **3** and the iodo-stilbene **7** provided the peripherally styryl functionalized star **S-TPEB** as a white solid in 49% isolated yield after column chromatography (cc). The 4-iodo-1,1'-biphenyl **8** was obtained in a one-pot *Sandmeyer*

procedure from the commercial 4-amino-1,1'-biphenyl.[19] A similar cross-coupling protocol as described above applied to **3** and **8** provided the peripherally phenyl functionalized star **P$_H$-TPEB** as a white crystalline solid in 83% yield after column chromatography. The hydroxyl-substituted star **P$_{OH}$-TPEB** was assembled in a divergent synthetic approach. Thus the 1,3,5-tri-ethynylbenzene **3** was further functionalized by applying a *Sonogashira* protocol with 1-bromo-4-iodobenzene to provide the extended start structure **4** in 79% isolated yield. A subsequent *Suzuki* coupling with the boronic acid **9** provided the hydroxyl-substituted star **P$_{OH}$-TPEB** which was isolated as hardly soluble white solid in a poor yield of 10% after tedious purification by cc and recycling gel-permeation-chromatography.

All star-type structures and precursors were characterized by ^{1}H- and ^{13}C-NMR spectroscopy and by mass spectrometry. The identity of **P$_H$-TPEB** was further corroborated by its solid state structure. Slow evaporation of a diluted chloroform sample provided single crystals suitable for X-ray analysis. The solid-state structure of **P$_H$-TPEB,** synthetic protocols of all new chemical structures and the description of the preparation of the PTCDI/melamine network and its modification by the star molecules are provided in the ESI.
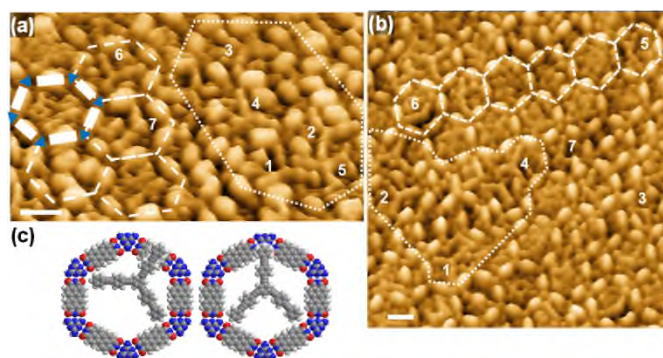

Fig. 2 High resolution STM images in 3D representation of PTCDI-melamine networks on Au(111)/mica after exposure to solutions of **S-TPEB** (a) and **PE-TPEB** (b). To guide the eye some intact cells are marked by white hexagons. Areas lacking the network structure are framed by dotted lines. Some of the **S-TPEB** and **PE-TPEB** molecules discussed in more detail in the text are labelled by numbers. (c) Models of **PE-TPEB** trapped in a network pore. Scale bars: 2 nm.

In high resolution STM images (Fig. 2) of network modified Au(111) substrates exposed to either **PE-TPEB** or **S-TPEB** all components are straightforwardly identified. As for the native network, PTCDI and melamine molecules appear as bright elliptic protrusions and dark vertices, respectively. The star molecules are even imaged at submolecular resolution as illustrated by those labelled by numbers (1-5 in Fig. 2a, 1-2 in Fig. 2b) which exhibit trigonal shapes composed of 7 protrusions, in accordance with the number of benzene rings in **PE-TPEB** and **S-TPEB**. In both images of Fig. 2 areas are seen where the network structure is intact and where the network has defects such as merged pores or irregularly arranged PTCDI-melamine strands. There is a clear preference for the star molecules to adsorb in areas lacking the network structure. This is confirmed by images which show an intact network on an extended scale (Fig. ESI3a). The trigonal shape of the star molecules is only discernible at defects (highlighted by the encircled areas in Fig. ESI3a). A closer look at the images of Fig. 2 reveals that the appearance of the star molecules varies substantially. While some **PE-TPEB** (e.g. 1-3 in Fig. 2a) and **S-TPEB** (1,2 in Fig. 2b) molecules exhibit their complete

shape, i.e., seven protrusions arising from the benzene rings, others appear truncated (e.g. 4-7 in Fig. 2a, 3-7 in Fig. 2b). Specifically, the **PE-TPEB** and **S-TPEB** molecules in an intact network pore (e.g. 6-7 in Fig. 2a, 5-7 in Fig. 2b) are always deviating from the threefold symmetry with one arm shortened or even completely missing. While the long arms usually point towards melamine there is, in agreement with observations on other systems involving ethynylene moieties,[17] significant flexibility in the geometry as in some cases the arms point to melamines positioned at an angle of 120° of the hexagonal pore in other cases they point to those positioned at 180°.

One obvious interpretation for observing truncated stars is that these are incomplete molecules present as impurity in the solution. However, we exclude this as in adsorption experiments without the network truncated molecules have never been observed. Instead, our explanation is that, consistent with the fact that most pores are empty, the **S-TPEB** and **PE-TPEB** molecules are too large to be accommodated by a pore. Due to the confined geometry the molecules can adsorb onto the metal substrate with at most two arms and the third arm is dangling across the pore boundary as illustrated in Fig. 2c which depicts models of **PE-TPEB** in configurations as seen in pores labelled 3 and 6 in Fig. 2b Analogously, in the case of damaged network pores truncated shapes would be indicative of interfering star molecules with two arms crossing. Whether this lack of imaging contrast can be explained by thermal motion of the weakly interacting arm or an electronic effect remains unclear at present.

Before turning to the smaller **P_{H/OH}-TPEB** stars a few additional points are worth noting. Firstly, the highly defective networks as shown in Fig. 2 are not representative of the quality achievable by the solution based preparation of the supramolecular network. They were deliberately chosen to illustrate the adsorption behaviour of **S-TPEB** and **PE-TPEB**. As exemplified by Figure 3a and discussed in detail elsewhere[14] networks of high structural quality can be prepared over extended areas. Secondly, the defects form during the synthesis of the network and are not due to exposure of the network to the star molecules. Thirdly, the Au reconstruction[20] is not lifted upon formation of the network and subsequent exposure to the star molecules as evidenced by the stripe-like contrast variations seen in Fig. ESI3a and in agreement with UHV studies of the melamine/PTCDI network[13]. Compared to the adsorbate free Au(111) surface[13, 21], there is, however, a significant difference in the periodicity of the structure. As known from other studies[22, 23] the reconstructed surface can be substantially altered by molecular adsorbates. In the present case an average value of about 70 Å is measured, i.e., a larger $24\times\sqrt{3}$ structure compared to the $22\times\sqrt{3}$ unit cell of the clean Au(111) surface. Furthermore, the length varies between 22 and 25 times the Au-Au distance. Interestingly, the periodicities of the reconstruction and the network are not matching as detailed in the ESI and illustrated by Fig. ESI3b. The relationship between network and substrate periodicity observed here is different from the epitaxial one found in experiments under ultrahigh vacuum (UHV) reported earlier which consists of a combination of hexagonal and parallelogram pore geometries.[13] The reason for this difference is not clear at present but, given the variability of the gold reconstruction, it might be the consequence of the rather different interfacial kinetics and energetics of the liquid and UHV environments.

For **P_{H/OH}-TPEB** a very different result is obtained compared to **PE-TPEB** and **S-TPEB** which exceed the size of the network pore. The complete star molecules are clearly seen in the STM

images of Fig. 3 (**P_{OH}-TPEB**) and Fig. ESI4 (**P_H-TPEB**), thus, proving that these molecules fit into the pores. There is, however, a decisive difference between **P_H-TPEB** and **P_{OH}-TPEB**. Comparison of the images of both molecules reveals that the fraction of network pores where star molecules are seen is very low for the former (encircled pores in Fig. ESI4), whereas for the latter, the stars are present in the overwhelming majority of pores. However, this does not mean that there is a difference in coverage. Rather it arises from a difference in the dynamics of the molecule. As detailed in a forthcoming publication, **P_H-TPEB** exhibits mobility on a timescale short compared to the time resolution of STM whereas for **P_{OH}-TPEB** motion is slowed down due to the three OH groups which can be expected to result in stronger interactions with the network and/or the substrate than **P_H-TPEB** due to hydrogen bonding and/or dipole interactions.
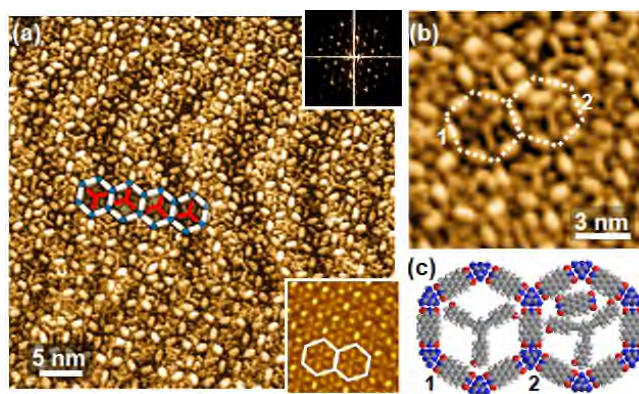

Fig. 3 STM images of PTCDI-melamine networks onm Au(111)/mica after exposure to **P_{OH}-TPEB**. (a) As a guide to the eye a few pores with stars are highlighted. Insets show Fourier transform of image (top right) and a section of the Fourier filtered image (bottom right). (b) High resolution image with two pores marked whose structural models are shown in (c).

Despite the high degree of pore filling and the **P_{OH}-TPEB** molecules fitting entirely into the pore, thus, maximising the interaction with the substrate, the Au surface, like for **PE-TPEB** and **S-TPEB**, remains reconstructed as seen in Fig. 3a. This is in agreement with other studies on extended aromatic systems for which the persistence of the herringbone reconstruction has been observed as well[10, 22, 24].

Analysing the large scale image of Fig. 3a the sharp spots seen in the Fourier transform (inset top right) confirm that the structural quality of the supramolecular template is not affected by the adsorption of the star molecule. The Fourier filtered image (inset, bottom right) yields a spot in the centre of the pore surrounded by a sixfold pattern which is aligned with the melamine vertices of the network. This pattern reflects the statistical occupation of the two positions schematically shown in Fig. 1a which are energetically equivalent due to the symmetry of the system..

A close look at the high resolution images like the one depicted in Fig. 3b, reveals additional features. Besides the dominating adsorption geometry where the molecule retains it symmetric star shape and all three arms point towards the melamine vertices (e.g. pore 1), the geometry of the **P_{OH}-TPEB** molecule is distorted in some of the pores with one arm pointing towards a PTCDI unit of the network (pore 2). In all these cases there is a pronounced additional protrusion which, based on the shape and imaging contrast, is reasonable to assume to be a PTCDI molecule. While a compartment defined by an undistorted star

molecule is too small to accommodate a PTCDI molecule, widening the angle between two arms by deformation of the ethynylene units allows the PTCDI to fit in as illustrated in the model of Fig. 3d. In this context it is worth noting that for a network such as the one shown in Fig. 3b which exhibits a high structural perfection we do not observe PTCDI molecules trapped in the pores prior to the adsorption of the star molecules. However, in the STM images the appearance of the pores can vary to some extent. For a small fraction the measured height difference between the PTCDI molecules of the network and the pore area is different from the other pores or streaky features are observed such as the one seen in the bottom of the STM image of Fig. 1a. This suggests that residual PTCDI molecules are present in some pores after the network preparation which, however, are too mobile to be resolved by STM. Their presence is only revealed after being locked into place by the adsorption of a star molecule

Conclusions

The experiments described above identify a strategy and the conditions for an iterative approach to ultraprecise two dimensional structures. A primary template generated by bottom-up self-assembly defines the positioning of another molecular entity which further reduces dimensions through partitioning of a pore. To achieve high yield and well defined compartmentation the molecule must fully fit into the pore.

Compared to a similar approach taken in a UHV experiment[25] where partitioning of pores is accomplished by three non-covalently interacting molecules, the strategy presented here using a single molecule provides higher flexibility in the design. Notably, going beyond the simple threefold symmety of the star molecule by modifying the geometry and/or introducing functionality and/or chirality to subpores, which can be envisaged to be different for each one, a new level of control at this small length scale opens up. Furthermore, partitioning by a purely covalent structure is also beneficial for the stability of the systems required in subsequent steps of a hierarchical assembly process.

Notes and references

[a] EaStCHEM School Chemistry, University of St Andrews, North Haugh, St Andrews,United Kingdom. E-mail:mb45@st-andrews.ac.uk
[b] Department of Chemistry, University of Basel, St. Johannsring 19, CH-4056 Basel, Switzerland. E-mail: marcel.mayor@unibas.ch
[c] Permanent address: Institute of Experimental Physics, University of Wroclaw, Pl. M. Borna 9, 50-204 Wroclaw, Poland.
[d] Institute for Nanotechnology, Karlsruhe Institute of Technology (KIT), P.O.Box 3640, D-76021 Karlsruhe, Germany.
[e] Lehn Institute of Functional Materials (LIFM), Sun Yat-Sen University (SYSU), Xingang Rd. W., Guangzhou, China.
†Electronic Supplementary Information (ESI) available: Experimental methods, X-ray crystal structure of P_H-TPEB and additional STM images of PTCDI-melamine networks exposed to S-TPEB and P_H-TPEB. See DOI: 10.1039/xxxx

1. J. Elemans, S. B. Lei and S. De Feyter, *Angew. Chem. Int. Ed.*, 2009, **48**, 7298-7332; A. G. Slater, P. H. Beton and N. R. Champness, *Chem. Sci.*, 2011, **2**, 1440-1448; L. Bartels, *Nat. Chem.*, 2010, **2**, 87-95; J. V. Barth,

Annu. Rev. Phys. Chem., 2007, **58**, 375-407; T. R. Eaton, D. M. Torres, M. Buck and M. Mayor, *CHIMIA*, 2013, **67**, 222-226.
2. S. Stepanow, M. Lingenfelder, A. Dmitriev, H. Spillmann, E. Delvigne, N. Lin, X. B. Deng, C. Z. Cai, J. V. Barth and K. Kern, *Nature Mat.*, 2004, **3**, 229-233; J. Čechal, C. S. Kley, T. Kumagai, F. Schramm, M. Ruben, S. Stepanow and K. Kern, *J. Phys. Chem. C*, 2013, **117**, 8871-8877.
3. A. Langner, S. L. Tait, N. Lin, C. Rajadurai, M. Ruben and K. Kern, *Proc. Natl. Acad. Sci. USA*, 2007, **104**, 17927-17930; P. A. Staniec, L. M. A. Perdigão, A. Saywell, N. R. Champness and P. H. Beton, *ChemPhysChem*, 2007, **8**, 2177-2181; K. Tahara, K. Inukai, J. Adisoejoso, H. Yamaga, T. Balandina, M. O. Blunt, S. De Feyter and Y. Tobe, *Angew. Chem. Int. Ed.*, 2013, **52**, 8373-8376; Y. B. Li, Z. Ma, K. Deng, S. B. Lei, Q. D. Zeng, X. L. Fan, S. De Feyter, W. Huang and C. Wang, *Chem. Eur. J.*, 2009, **15**, 5418-5423.
4. M. T. Räisänen, A. G. Slater, N. R. Champness and M. Buck, *Chem. Sci.*, 2012, **3**, 84-92.
5. J. Adisoejoso, K. Tahara, S. Okuhata, S. Lei, Y. Tobe and S. De Feyter, *Angew. Chem. Int. Ed.*, 2009, **48**, 7353-7357.
6. R. Madueno, M. T. Räisänen, C. Silien and M. Buck, *Nature*, 2008, **454**, 618-621.
7. C. Silien, M. T. Räisänen and M. Buck, *Angew. Chem. Int. Ed.*, 2009, **48**, 3349-3352.
8. C. Silien, M. T. Räisänen and M. Buck, *Small*, 2010, **6**, 391-394.
9. M. Stohr, M. Wahl, H. Spillmann, L. H. Gade and T. A. Jung, *Small*, 2007, **3**, 1336-1340.
10. S. D. Ha, B. R. Kaafarani, S. Barlow, S. R. Marder and A. Kahn, *J. Phys. Chem. C*, 2007, **111**, 10493-10497.
11. P. Szabelski, S. De Feyter, M. Drach and S. B. Lei, *Langmuir*, 2010, **26**, 9506-9515; P. Szabelski, W. Rzysko, T. Panczyk, E. Ghijsens, K. Tahara, Y. Tobe and S. De Feyter, *RSC Advances*, 2013, **3**, 25159-25165; Z. Mu, L. Shu, H. Fuchs, M. Mayor and L. Chi, *J. Am. Chem. Soc.*, 2008, **130**, 10840-10841.
12. J. A. Theobald, N. S. Oxtoby, M. A. Phillips, N. R. Champness and P. H. Beton, *Nature*, 2003, **424**, 1029-1031.
13. F. Silly, A. Q. Shaw, G. A. D. Briggs and M. R. Castell, *Appl. Phys. Lett.*, 2008, **92**, 023102.
14. I. Cebula, M. T. Räisänen, R. Madueno, B. Karamzadeh and M. Buck, *Phys. Chem. Chem. Phys.*, 2013, **15**, 14126-14127.
15. V. V. Korolkov, N. Mullin, S. Allen, C. J. Roberts, J. K. Hobbs and S. J. B. Tendler, *Phys. Chem. Chem. Phys.*, 2012, **14**, 15909-15916.
16. T. Takeda and Y. Tobe, *Chem. Commun.*, 2012, **48**, 7841-7843; S. Toyota, T. Yamamori and T. Makino, *Tetrahedron*, 2001, **57**, 3521-3528; G. Jeschke, M. Sajid, M. Schulte, N. Ramezanian, A. Volkov, H. Zimmermann and A. Godt, *J. Am. Chem. Soc.*, 2010, **132**, 10107-10117.
17. D. Heim, D. Écija, K. Seufert, W. Auwärter, C. Aurisicchio, C. Fabbro, D. Bonifazi and J. V. Barth, *J. Am. Chem. Soc.*, 2010, **132**, 6783-6790; D. Ecija, S. Vijayaraghavan, W. Auwärter, S. Joshi, K. Seufert, C. Aurisicchio, D. Bonifazi and J. V. Barth, *ACS Nano*, 2012, **6**, 4258-4265.
18. N. M. Jenny, M. Mayor and T. R. Eaton, *Eur. J. Org. Chem.*, 2011, 4965-4983.
19. E. A. Krasnokutskaya, N. I. Semenischeva, V. D. Filimonov and P. Knochel, *Synthesis-Stuttgart*, 2007, 81-84.
20. U. Harten, A. M. Lahee, J. P. Toennies and C. Wöll, *Phys. Rev. Lett.*, 1985, **54**, 2619-2622; A. R. Sandy, S. G. J. Mochrie, D. M. Zehner, K. G. Huang and D. Gibbs, *Phys. Rev. B*, 1991, **43**, 4667-4687.
21. C. Wöll, S. Chiang, R. J. Wilson and P. H. Lippel, *Phys. Rev. B*, 1989, **39**, 7988-7991.
22. F. Rossel, P. Brodard, F. Patthey, N. V. Richardson and W.-D. Schneider, *Surf. Sci.*, 2008, **602**, L115-L117.
23. J. T. Sun, L. Gao, X. B. He, Z. H. Cheng, Z. T. Deng, X. Lin, H. Hu, S. X. Du, F. Liu and H. J. Gao, *Phys. Rev. B*, 2011, **83**, 115419.
24. C. B. France, P. G. Schroeder, J. C. Forsythe and B. A. Parkinson, *Langmuir*, 2003, **19**, 1274-1281; F. Silly, A. Q. Shaw, M. R. Castell and G. A. D. Briggs, *Chem. Commun.*, 2008, 1907-1909; Y. Y. Lo, J. H. Chang, G. Hoffmann, W. B. Su, C. I. Wu and C. S. Chang, *Jap. J. Appl. Phys.*, 2013, **52**, 101601-101606.
25. D. Kühne, F. Klappenberger, W. Krenner, S. Klyatskaya, M. Ruben and J. V. Barth, *Proc. Natl. Acad. Sci. USA*, 2010.